Backfolding Corrections for Freely Jointed Chains in Self Consistent Field Lattice Models

Philip P. Simon and Harry J. Ploehn*

Department of Chemical Engineering, Swearingen Engineering Center, University of South Carolina, Columbia, South Carolina 29206

Received February 5, 1998; Revised Manuscript Received June 4, 1998

ABSTRACT: This work presents a methodology to exclude backfolding (overlapping of sequential segments) in lattice models for freely jointed linear and branched polymer molecules. The introduction of conditional weighting factors that account for occupancy of sites by neighboring segments leads to the generation of new recursive relationships to compute the chain weighting factors that quantify configurational probabilities. Calculations are performed for representative linear and branched homopolymers and copolymers. The results indicate that the allowance or prohibition of backfolding has a significant effect on the predicted structure of adsorbed polymer layers, especially the surface volume fractions and adsorbed amounts, at least when the segmental adsorption energy is relatively low.

I. Introduction

The Flory theory of polymer solution thermodynamics[1] derives the free energy of mixing of a polymer in a solvent from its enthalpy and configurational entropy of mixing. The configurational entropy corresponds to the number of ways a polymer molecule may be placed in a lattice. In a lattice of coordination number z, the entropy is calculated by placing one segment of the molecule at a time into the lattice while accounting for the presence of the nearest neighbor previously placed. Although the molecule is modeled as a freely-jointed chain (capable of turning in any random direction), the theory does not permit two segments that are immediate neighbors of a given segment to occupy the same site. In this sense, the number of conformations

$$\Omega_i^* = \frac{(r_i n_i)!}{n_i!}\left(\frac{z}{z-1}\right)^{n_i}\left(\frac{z-1}{r_i n_i}\right)^{n_i(r_i-1)} \approx \frac{(r_i n_i)!}{n_i!}\left(\frac{z-1}{r_i n_i}\right)^{n_i(r_i-1)} \quad (1)$$

does not include *direct backfolding* in spatially homogeneous systems. Here n_i is the number of molecules of type i, r_i is the number of segments in molecule i, and z is the coordination number of the lattice.

Self-consistent field (SCF) lattice models for polymeric systems have extended the Flory lattice concept to inhomogeneous systems. The homopolymer-solvent model introduced by Scheutjens and Fleer[2] was the prototype for a variety of SCF lattice models developed recently, including copolymer-solvent mixtures,[3] pure polymers at surfaces,[4] variable volume systems,[5] and free surface of blends.[6] However, unlike the original Flory polymer solution theory, these models have inherently introduced backfolding through the form of the recursive formula used to compute configurational probabilities. The models maintain internal consistency by using a version of the Flory formula

$$\Omega_i^* = \frac{(r_i n_i)!}{n_i!}\left(\frac{z}{r_i n_i}\right)^{n_i(r_i-1)} \quad (2)$$

that allows overlapping of sequential segments (i.e., backfolding). The backfolding assumption in these models is embodied in the *site-weighted average* ($\langle\cdot\rangle$) recursive formula that assumes that all of the z sites neighboring a segment are available for placing the next segment. Although the magnitude of the error introduced by this assumption for linear molecules is uncertain, it is the same for all segments except the chain ends. In a branched molecule, the placement of several segments adjacent to the branching segment multiplies the error introduced by allowing multiple overlaps. Furthermore, the error will vary among the segments of a chain since only some of them are branch segments. Consequently, the error varies with the architecture of the molecule. An estimate of these errors may be important to our understanding of the relationship between polymer architecture and solution or interfacial microstructure.

Leermakers *et al.*[7] extended the SCF model for a two-tailed branch molecule (one branch point) using the freely-jointed chain with backfolding (known as a first-order Markov chain) as well as a rotational isomeric scheme (RIS). The RIS inherently eliminates backfolding because it restricts the values of the bond angle between segments i and $i+1$ based on the value of the bond angle between segments $i-1$ and i. Actually, this approach prevents the overlapping of four consecutive segments of the same chain in addition to imposing bond-angle restrictions. Leermakers *et al.*[7] compare the use of first-order Markov statistics with the RIS and find significant differences in the structure predicted by the two schemes for small molecules. van der Linden *et al.*[8] developed a chain stiffness model that can be used to eliminate backfolding in the case of the cubic lattice. This model classifies three possible sequences of three segments on a chain in a cubic lattice: a 90° perpendicular step, a 180° straight step, and a 0° backfolding step. Each step is weighted by its associated energy penalty. By adjusting the values of these energy penalties, chains can be restricted from taking certain steps. One eliminates backfolding by setting the associated energy penalty to infinity, which results in a zero weighting factor. The weighting factors are normalized to add up to one at each site. The equations derived in this approach take advantage of the rectangular cell arrangement in a cubic lattice. In a hexagonal

S0024-9297(98)00170-3 CCC: $15.00 © 1998 American Chemical Society
Published on Web 08/08/1998

lattice, the step sequences are more numerous than the three listed above. Consequently, a new derivation is necessary to extend this chain stiffness model to the hexagonal lattice.

In this paper, we examine the effect of preventing direct backfolding in a freely jointed chain model of a polymer molecule. We define backfolding as the occupation of a site by two or more immediate neighbors of the same segment. In a linear chain, our correction to backfolding amounts to restricting the overlapping of three consecutive segments in the chain without imposing any restrictions on the bond angles. This approach is independent of the geometry of the lattice, whether it is cubic or hexagonal. The use of the appropriate coordination number and the number of sites in neighboring layers incorporates the lattice effects. This correction permits examination of the effect of backfolding on structure in polymer-solvent mixtures for various linear and branched chain architectures.

II.Theory

II.A. Partition Function. This work represents an extension of the model of Evers *et al.*[3] Consequently, we retain and extend the notation used in this reference. The reader should consult this reference for the full description of the theory.

The grand canonical partition function

$$\Xi(\{\mu_i\},M,L,T) = \sum_{\text{all}\{n_i^c\}} Q(\{n_i^c\},M,L,T)\exp\left(\sum_i n_i\mu_i/kT\right) \quad (3)$$

governs the distribution of molecules of type i on a lattice of M layers with L sites per layer. The system contains n_i^c molecules of type i in configuration c ($n_i = \sum_c n_i^c$). At equilibrium, the chemical potentials μ_i are constant. We maximize the grand partition function Ξ for the polymer system with the constraint of full occupancy of all lattice sites in order to obtain the most probable distribution of conformations. The canonical partition function

$$Q = Q^*\left(\frac{\Omega}{\Omega^*}\right)\exp[-(U-U^*)/kT] \quad (4)$$

consists of the entropic combinatorial factor Ω and the energy-weighted Boltzmann factor. The quantities denoted with the asterisk are reference values defined previously.[3] The form of combinatorial portion of the partition function determines whether backfolding is allowed or excluded. We retain the Bragg−Williams or random-mixing approximation[2] in the site-weighted averaging of the interaction energy of the segments in the lattice, which assumes that the interaction energy of a segment is a function of the average volume fraction of the species in the layers immediately surrounding the segment. In the following section, we derive appropriate combinatorial terms consistent with the exclusion of backfolding.

II.B. Combinatorial Degeneracy. The following example illustrates the effect of segment backfolding on the combinatorial factor Ω. Scheutjens and Fleer[2] define a conformation by specifying the layer numbers associated with each segment in the molecule. Consider the conformations for two architectures of a six-segmented molecule shown in Figure 1. If backfolding were allowed, the number of ways that the conformation can exist for both molecules is

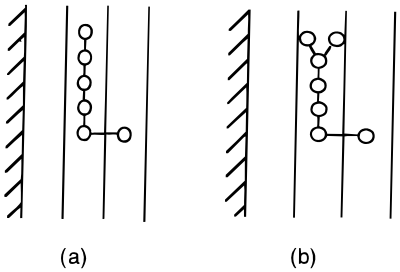

Figure 1. Conformation of two six-segmented molecules: (a) linear molecule, (b) branched molecule.

$$\omega = Lz\lambda_0 z\lambda_0 z\lambda_0 z\lambda_0 z\lambda_1 = Lz^5\lambda_0{}^4\lambda_1 \quad (5)$$

where L is the number of sites per lattice layer, z is the lattice coordination number (6 for cubic and 12 for hexagonal), and λ_i is the fraction of nearest neighbor sites in any layer relative to a given site. The subscript indicates relative position: $i = 0$ represents a site in the same layer as the given site, and $i = \pm 1$ represents adjacent layers. Note that ω is the same for both the linear and the branched polymer shown in Figure 1: configurational entropy depends on the number of segments in each layer and is *independent* of the architecture of the molecule. This result is counterintuitive and ensues from our ignoring the sites excluded by nearest-neighbor segments.

A more accurate representation of the configurational degeneracy for the linear polymer would be

$$\omega = Lz\lambda_0(z\lambda_0-1)(z\lambda_0-1)(z\lambda_0-1)z\lambda_1 = Lz^5\lambda_0\lambda_0'^3\lambda_1 \quad (6)$$

where the terms λ_j' are defined by

$$\lambda_j' \equiv \lambda_j - \frac{1}{z} \quad (7)$$

By the same reasoning, the configurational degeneracy of the given configuration of the branched molecule is

$$\omega = Lz\lambda_0(z\lambda_0-1)(z\lambda_0-2)(z\lambda_0-1)z\lambda_1 = Lz^5\lambda_0\lambda_0'^2\lambda_0''\lambda_1 \quad (8)$$

in which

$$\lambda_j'' \equiv \lambda_j - \frac{2}{z} \quad (9)$$

In this way the configurational entropy becomes dependent on the molecular architecture. The combinatorial term can then be written in the same form as in Evers *et al.*[3]

$$\Omega = (L!)^M\prod_{i,c}\frac{[\lambda'^c(Z/L)^{r_i-1}]^{n_i^c}}{n_i^c!} \quad (10)$$

where λ'^c is a product involving λ_j, λ_j', and λ_j'' for a given conformation c of molecule i.

Next, we need to develop a consistent expression for Ω_i^* in

$$\Omega^* = \prod_i \Omega_i^* \tag{11}$$

which is usually taken from Flory's expression[1] for linear molecules. For a molecule that is longer than two segments with three-node (as in Figure 1b) and four-node branching segments, the combinatorial term for a homogeneous polymer-solvent mixture can be derived as a function of the architecture as

$$\Omega_i^* = \frac{(r_i n_i)!}{n_i!}\left(\frac{z}{z-1}\right)^{n_i}\left(\frac{z-1}{r_i n_i}\right)^{n_i(r_i-1)} \times \left(\frac{z-2}{z-1}\right)^{n_i(b_{3i}+b_{4i})}\left(\frac{z-3}{z-1}\right)^{n_i b_{4i}} \tag{12}$$

where n_i is the number of molecules of molecule type i with r_i total segments, and b_{3i} and b_{4i} are the number of three-node and four-node branch segments. Combining eqs 10 to 12 produces

$$\ln\frac{\Omega}{\Omega^*} = \sum_{i,c} n_i^c \ln\left[\left(\frac{z}{z-1}\right)^{r_i-2}\left(\frac{z-1}{z-2}\right)^{b_{3i}+b_{4i}}\left(\frac{z-1}{z-3}\right)^{b_{4i}}\left(\frac{L\lambda'^c}{r_i n_i^c}\right)\right] \tag{13}$$

proportional to the configurational entropy.

II.C. Number Distribution of Conformations. Minimizing the free energy or maximizing Ξ determines the equilibrium distribution of conformations. The details of this procedure follow exactly as in the work of Evers *et al.*[3] The number distributions of configurations can be represented as

$$\frac{n_i^c}{L} = C_i'\lambda'^c\prod_{z,A} G_A(z)^{r_{Ai}^c(z)} \tag{14}$$

which is identical to eq 17 of Evers *et al.*[3] with the notable difference that primes on λ'^c and the normalization constant C_i' indicate that the counting excludes the sites occupied by the nearest-neighbor segments. Here $G_A(z)$ is the free segment weighting factor of segment type A, and $r_{Ai}^c(z)$ is the number of A-type segments of molecule i in layer z if the molecule is in conformation c. Maximizing Ξ determines the normalization constant in eq 14, giving

$$\ln C_i' = \ln\left(\frac{z}{z-1}\right)^{r_i-2}\left(\frac{z-1}{z-2}\right)^{b_{3i}+b_{4i}}\left(\frac{z-1}{z-3}\right)^{b_{4i}} + \frac{\mu_i - \mu_i^*}{kT} - 1 + \sum_A \frac{r_{Ai}^d\, u_A^{ref}}{kT} + \frac{\partial U^*/kT}{\partial n_i} - \ln r_i \tag{15}$$

where u_A is the self-consistent field for segments of type A. The superscript ref denotes an arbitrary reference state. The first term in eq 15 arises due to the exclusion of backfolding and makes the normalization constant depend explicitly on molecular architecture. The value of C_i' depends on the choice of the reference state. We follow the approach of Evers *et al.*[3] by selecting a reference state such that $G_A(z)$ are all unity in the bulk (homogeneous) solution.

II.D. Chain End Distribution Functions. As stated by Evers *et al.*,[3] the next objective is to compute the segment density distributions $\phi_A(z)$ without explicit enumeration of all molecular configurations. Again, we have adopted and extended their notation.

To begin, eq 14 may be written as

$$\frac{n_i^c}{L} = C_i'\lambda'^c G_i^c \tag{16}$$

where $G_i^c = \prod_{z,A} G_A(z)^{r_{Ai}^c(z)}$ is the product of free segment weighting factors for a molecule of type i in conformation c. The equilibrium distribution of segment densities includes contributions from all possible conformations of the molecules. By summing over all possible conformations, the total number of molecules of type i may be expressed as

$$\frac{n_i}{L} = C_i'\sum_c \lambda'^c G_i^c \tag{17}$$

The summation term defines the *chain weighting factor* $G_i(r_i|1)$

$$G_i(r_i|1) = \sum_z G_i(z,r_i|1) = \sum_c \lambda'^c G_i^c \tag{18}$$

expressing the statistical weight of all conformations of molecules i in the lattice. The statistical weight of molecules i ending with the last segment r_i in layer z, known as the *chain end distribution function*, $G_i(z,r_i|1)$, is defined by

$$G_i(z,r_i|1) = \sum_{c(z,r_i)} \lambda'^c G_i^c \tag{19}$$

The notation $c(z,r_i)$ indicates that the sum includes only those conformations that bring the r_i^{th} segment to layer z. This equation corresponds to eq 23 in Evers *et al.*[3] We should not forget that λ'^c and G_i^c are products over segments numbered from 1 to r_i.

In order to exclude backfolding, we must define additional weighting factors not required in previous lattice models. We define *conditional weighting factors*

$$G_i(z-1, r_i-1|1;[z, r_i]) = \sum_{c(z-1,r_i-1;z,r_i)} \lambda'^c(r_i-1|1)G_i^c(r_i-1|1)$$

$$G_i(z, r_i-1|1;[z, r_i]) = \sum_{c(z,r_i-1;z,r_i)} \lambda'^c(r_i-1|1)G_i^c(r_i-1|1)$$

$$G_i(z+1, r_i-1|1;[z, r_i]) = \sum_{c(z+1,r_i-1;z,r_i)} \lambda'^c(r_i-1|1)G_i^c(r_i-1|1) \tag{20}$$

for subchains of length $r_i - 1$, similar to $G_i(z,r_i|1)$ defined in eq 19. The notation $c(z-1,r_i-1;z,r_i)$ represents the set of conformations having segment $r_i - 1$ in layer $z - 1$ and segment r_i in layer z. The quantity $G_i(z-1,r_i-1|1;[z,r_i])$ represents the statistical weight of subchains containing $r_i - 1$ segments beginning with segment 1 and ending with segment $r_i - 1$ in layer $z - 1$, summed over all conformations having segment $r_i -$

1 in layer $z-1$ and segment r_i in layer z. The notation $[z,r_i]$ reminds us that the subchain of interest *does not* include segment r_i in layer z, although the summation includes all conformations having segment r_i in layer z. The fact that the imposed condition relates to the next nearest segment and not to any other segments along the chain will become important when we consider multiple conditions that must be imposed in the case of branched molecules.

The chain end distribution function $G_i(z,r_i|1)$ can be expressed recursively in terms of the distribution functions of subchains ending in the (r_i-1)th segment, i.e., the conditional weighting factors. We break down the summation in eq 19 into three parts containing subchains ending with the (r_i-1)th segment in layers $z-1$, z, and $z+1$. From each of these, we extract the terms in the product $\lambda'^{c}G_i^{c}$ that correspond to the r_ith segment. Using the definitions of the conditional weighting factors, we have

$$G_i(z,r_i|1) = G_i(z,r_i)\begin{Bmatrix}\lambda_{-1}G_i(z-1,\,r_i-1|1;[z,r_i])\\ +\,\lambda_0 G_i(z,r_i-1|1;[z,r_i])\\ +\,\lambda_1 G_i(z+1,r_i-1|1;[z,r_i])\end{Bmatrix}$$

$$= G_i(z,r_i)\langle G_i(z,r_i-1|1;[z,r_i])\rangle \qquad (21)$$

where the λ_i coefficients of the conditional weighting factors reflect the fraction of sites neighboring segment r_i located in layer z. The quantity $G_i(z,r_i)$ is the free segment weighting factor, equal to $G_A(z)$ if segment r_i of molecule i is of type A and is located in layer z. The angle bracket notation in eq 21 is a convenient standard for representing the site-weighted average over adjacent layers.

Modified coefficients of the type λ_i' do not appear in eq 21 because the r_ith segment is the last segment: we do not need to account for sites occupied by segments following it. However, to properly exclude backfolding, recursive equations for conditional weighting factors for all subchains must contain λ_i' terms. This can be illustrated by expanding one of the conditional weighting factors for a subchain of length s into conformation sets of a subchain ending in segment $s-1$. For instance,

$$G_i(z,s|1;[z+1,\,s+1]) = G_i(z,s)\begin{Bmatrix}\lambda_{-1}G_i(z-1,s-1|1;[z,s])\\ +\,\lambda_0 G_i(z,s-1|1;[z,s])\\ +\,\lambda_1' G_i(z+1,s-1|1;[z,s])\end{Bmatrix}$$

$$= G_i(z,s)\langle G_i(z,s-1|1;[z,s])\rangle_{z+1,s+1} \qquad (22)$$

gives the conditional weighting factor for a subchain containing s segments beginning at segment 1 and ending with segment s in layer z, subject to the condition that segment $s+1$ is in layer $z+1$. This equation accounts for occupancy of segment $s+1$ of the site in layer $z+1$ by furnishing segment $s-1$ with only $z\lambda_1'$ sites in layer $z+1$. Thus we have λ_1' as the coefficient of third term on the right side of eq 22. The angle bracket notation can be used again with the subscript indicating the site and segment responsible for the constraint, as well as the term in the equation that requires a modified coefficient.

The two related conditional weighting factors required for recursion can be written as

$$G_i(z,s|1;[z,s+1]) = G_i(z,s)\begin{Bmatrix}\lambda_{-1}G_i(z-1,s-1|1;[z,s])\\ +\,\lambda_0' G_i(z,s-1|1;[z,s])\\ +\,\lambda_1 G_i(z+1,s-1|1;[z,s])\end{Bmatrix}$$

$$= G_i(z,s)\langle G_i(z,s-1|1;[z,s])\rangle_{z,s+1} \qquad (23)$$

and

$$G_i(z,s|1;[z-1,s+1]) = G_i(z,s)\begin{Bmatrix}\lambda_{-1}'G_i(z-1,s-1|1;[z,s])\\ +\,\lambda_0 G_i(z,s-1|1;[z,s])\\ +\,\lambda_1 G_i(z+1,s-1|1;[z,s])\end{Bmatrix}$$

$$= G_i(z,s)\langle G_i(z,s-1|1;[z,s])\rangle_{z-1,s+1} \qquad (24)$$

We also require three analogous recursion equations for chains beginning at segment r_i. The weighting factors for $s=1$ equal the free segment weighting factors. These expressions provide a pattern for recursive calculation of the conditional weighting factors for the end-segment s of any linear subchain.

The same concepts can be applied to develop recursive equations for the conditional weighting factors for branch point segments. These are given in Appendix I.

II.E. Composition Law. The chain weighting factor $G_i(r_i|1)$, defined by eq 18, quantifies the statistical weight of all molecules of type i by adding the weights of all chain ends r_i in every layer z. Since the weight of all conformations is independent of which segment is used for counting, we could just as well count any interior segment s. Denoting the chain weighting factor more generally as $G_i(r_i|s|1)$, it could be computed from

$$G_i(r_i|s|1) = \sum_z G_i(r_i|(z,s)|1) = \sum_z \sum_{c(z,s)} \lambda'^{c} G_i^{c} = \sum_c \lambda'^{c} G_i^{c} \qquad (25)$$

where $G_i(r_i|(z,s)|1)$ represents the weight of all chains having segment s in layer z. By analogy with eq 19, we denote $G_i(r_i|(z,s)|1)$ as the *chain segment distribution function* for the sth segment. This function exhibits inversion symmetry in that $G_i(r_i|(z,s)|1) = G_i(1|(z,s)|r_i)$.

A composition law must be used to calculate $G_i(r_i|(z,s)|1)$. If backfolding is allowed, then $G_i(r_i|(z,s)|1)$ equals the product of two conditional weighting factors for subchains of lengths s and r_i-s ending in layer z, divided by the free segment weighting factor $G_i(z,r_i)$ to avoid double-counting the joining segment. The composition law becomes more complicated when backfolding is not permitted because we must account for the fact that segments $s-1$ and $s+1$ cannot occupy the same site. From eq 21, the conditional weighting factor for a subchain of length s ending in layer z

$$G_i(z,s|1) = G_i(z,s)\begin{Bmatrix}\lambda_{-1}G_i(z-1,s-1|1;[z,s])\\ +\,\lambda_0 G_i(z,s-1|1;[z,s])\\ +\,\lambda_1 G_i(z+1,s-1|1;[z,s])\end{Bmatrix} \qquad (26)$$

includes contributions from subchains with segment $s-1$ in layers $z-1$, z, and $z+1$. Each of these terms must be multiplied by an appropriate conditional weighting factor for a subchain of length $r_i - s$ ending in layer z. For example, using the notation in eqs 22−24

$$\langle G_i(z,s+1|r_i;[z,s])\rangle_{z-1,s-1} = \begin{Bmatrix} \lambda'_{-1}G_i(z-1,s+1|r_i;[z,s]) \\ +\lambda_0 G_i(z,s+1|r_i;[z,s]) \\ +\lambda_1 G_i(z+1,s+1|r_i;[z,s]) \end{Bmatrix} \quad (27)$$

gives a site-weighted conditional weighting factor for $r_i - s$ length subchains. The modified coefficient of the first term accounts for the occupancy of a site in layer $z-1$ by another segment, namely, the $s-1$ segment from the first term in eq 26. Similar conditional weighting factors can be written for $r_i - s$ length subchains that correct for occupancy of sites in layers z and $z+1$. Multiplying each term in eq 26 by an appropriate conditional weighting factor similar to eq 27 produces

$$G_i(r_i|(z,s)|1) = G_i(z,s) \begin{Bmatrix} \lambda_{-1}G_i(z-1,\, s-1|1;[z,s])\langle G_i(z,s+1|r_i;[z,s])\rangle_{z-1,s-1} \\ +\lambda_0 G_i(z,s-1|1;[z,s])\langle G_i(z,s+1|r_i;[z,s])\rangle_{z,s-1} \\ +\lambda_1 G_i(z+1,\, s-1|1;[z,s])\langle G_i(z,\, s+1|r_i;[z,s])\rangle_{z+1,s-1} \end{Bmatrix} \quad (28)$$

as the composition law when backfolding is prohibited. Each angle bracket term represents a sum of site-weighted conditional weighting factors. Expanding these, each resulting term in the curly brackets is a product of two conditional weighting factors for two complementary subchains in which segments $s-1$ and $s+1$ do not overlap.

The expressions developed above apply to interior segments in linear chains or linear portions of branched chains. Expressions of the composition law for branching segments can be developed following the same reasoning. These expressions are given in Appendix II.

II.F. Volume Fraction Distributions. Volume fraction distributions of particular segments can be written as

$$\phi_i(z,s) = C'_i G_i(r_i|(z,s)|1) = C'_i \sum_{c(z,s)} \lambda'^{c} G_i^{c} \quad (29)$$

in terms of the normalization constant and the chain segment distribution function for segment s in a chain molecule of type i. Again, $c(z,s)$ denotes those conformations in which the sth segment of the molecule occurs in the layer z. G_i^c is the product of all the free segment weighting factors $G_A(z)$ for all the segments in molecule i, and λ'^c is the product of all λ_i associated with the conformation.

The volume fraction of component i in layer z is simply the sum of the segment volume fractions over all segments:

$$\phi_i(z) = \sum_{s=1}^{r_i}\phi_i(z,s) = C'_i\sum_{s=1}^{r_i} G_i(r_i|(z,s)|1) = C'_i\sum_{s=1}^{r_i}\sum_{c(z,s)} \lambda'^{c} G_i^{c} \quad (30)$$

II.G. Reference State. A spatially homogeneous mixture of the components ("bulk solution") serves as the reference state. In bulk, all $G_A(z)$ are unity for all species, and thus $G_i^c = \prod_{z,A} G_A(z)^{r^c{}_{Ai}(z)} = 1$. If backfolding were permitted, then $G_i(r_i|(z,s)|1) = \sum_{c(z,s)}\lambda^c G_i^c = 1$ because all z sites are available and all λ_i terms add to unity in equations such as eq 28. Substituting this into eq 30 fixes $C_i = \phi_i^b/r_i$ as the normalization constant for linear molecules. If backfolding is not permitted, then $G_i(r_i|(z,s)|1) = \sum_{c(z,s)}\lambda'^c G_i^c$ does not add to unity. However, this does not alter the field chosen for the reference state in eq 15.

The expressions for the conditional weighting factors for the linear segments in eqs 21 to 24 indicate that the first and last segments of a linear chain do not require correction for overlapping. Thus, for a linear molecule of r_i segments, only $r_i - 2$ internal segments require corrected coefficients. The sum of the λ'_i terms in eqs 23 and 24 for each of the internal segments adds to $(z-1)/z$ instead of unity. Since the free segment weighting factors are unity in the reference state, eqs 22 to 24 for the chain end distribution function and eq 28 for the chain segment distribution function yield a value of $[(z-1)/z]^{r_i-2}$ for linear molecules. Similarly, eqs I.1−I.5 in the Appendix I show that, in branched molecules, each branch segment introduces a factor of $(z-1)(z-2)/z^2$.

Under bulk conditions, when $G_A(z) = 1$, and the volume fractions equal ϕ_i^b, eq 30 becomes

$$C'_i = \frac{\phi_i^b}{r_i}\left(\frac{z-1}{z-3}\right)^{b_{4i}}\left(\frac{z-1}{z-2}\right)^{b_{4i}+b_{3i}}\left(\frac{z}{z-1}\right)^{r_i-2} \quad (31)$$

after rearrangement. The configurational entropy under bulk conditions, obtained by substituting from eqs 14 and 31 into eq 13, returns the same expression for the free energy of the system as eq I.3 of Evers *et al.*[3] The expressions for the chemical potential that result from the free energy are therefore identical to their eq I.8. In order to obtain the field u_A^{ref} associated with the reference state, we reduce eq 15 for the normalization constant using the expressions calculated above. We get the reference state potential with the same expression as eq 44 of Evers *et al.*[3]

Thus, the changes in the configurational entropy introduced through exclusion of backfolding, produces no change in the expressions for the chemical potential and the reference state field. This result is not surprising because we have consistently applied exclusion of backfolding in the homogeneous solution as well as the inhomogeneous solution.

II.H. Calculation Procedure. The conditional weighting factors defined in section II.D. can be divided into three basic types:

$$G_i^b(z,s|1) \equiv G_i(z,s|1;[z-1,s+1])$$

$$G_i^c(z,s|1) \equiv G_i(z,s|1;[z,s+1])$$

$$G_i^f(z,s|1) \equiv G_i(z,s|1;[z+1,s+1]) \quad (32)$$

in terms of simplified notation with superscripts b, c, and f denoting "backward", "central", and "forward" factors. These conditional weighting factors account for the presence of segment $s+1$ in the layers $z-1$, z,

and $z + 1$ when segment s is in layer z. The recursion eqs 22−24 can be expressed as

$$G_i^{\mathrm{f}}(z,s|1) = G_i(z,s)\{\lambda_{-1}G_i^{\mathrm{f}}(z-1,s-1|1) + \lambda_0 G_i^{\mathrm{c}}(z,s-1|1) + \lambda_1' G_i^{\mathrm{b}}(z+1,s-1|1)\}$$

$$G_i^{\mathrm{c}}(z,s|1) = G_i(z,s)\{\lambda_{-1}G_i^{\mathrm{f}}(z-1,s-1|1) + \lambda_0' G_i^{\mathrm{c}}(z,s-1|1) + \lambda_1 G_i^{\mathrm{b}}(z+1,s-1|1)\}$$

$$G_i^{\mathrm{b}}(z,s|1) = G_i(z,s)\{\lambda_{-1}' G_i^{\mathrm{f}}(z-1,s-1|1) + \lambda_0 G_i^{\mathrm{c}}(z,s-1|1) + \lambda_1 G_i^{\mathrm{b}}(z+1,s-1|1)\} \quad (33)$$

for chains beginning at segment 1 and ending at segment $s \geq 2$. For $s = 1$, all of the weighting factors equal the free segment weighting factor. Likewise, for chains beginning at segment r_i and ending at segment s, we have

$$G_i^{\mathrm{f}}(z,s|r_i) = G_i(z,s)\{\lambda_{-1}G_i^{\mathrm{f}}(z-1,s+1|r_i) + \lambda_0 G_i^{\mathrm{c}}(z,s+1|r_i) + \lambda_1' G_i^{\mathrm{b}}(z+1,s+1|r_i)\}$$

$$G_i^{\mathrm{c}}(z,s|r_i) = G_i(z,s)\{\lambda_{-1}G_i^{\mathrm{f}}(z-1,s+1|r_i) + \lambda_0' G_i^{\mathrm{c}}(z,s+1|r_i) + \lambda_1 G_i^{\mathrm{b}}(z+1,s+1|r_i)\}$$

$$G_i^{\mathrm{b}}(z,s|r_i) = G_i(z,s)\{\lambda_{-1}' G_i^{\mathrm{f}}(z-1,s+1|r_i) + \lambda_0 G_i^{\mathrm{c}}(z,s+1|r_i) + \lambda_1 G_i^{\mathrm{b}}(z+1,s+1|r_i)\} \quad (34)$$

for $s \leq (r_i - 1)$. When $s = r_i$, all of the weighting factors equal the free segment weighting factor. Since the forward, central, and backward weighting factors appear together in each recursion equation, it is convenient to program these as separate data structures. All six types of conditional weighting factors appear in the composition law, eq 28, rewritten as

$$G_i(r_i|(z,s)|1) = G_i(z,s)\begin{Bmatrix} \lambda_{-1}G_i^{\mathrm{f}}(z-1,s-1|1)\langle G_i(z,s+1|r_i;[z,s])\rangle_{z-1,s-1} \\ + \lambda_0 G_i^{\mathrm{c}}(z,s-1|1)\langle G_i(z,s+1|r_i;[z,s])\rangle_{z,s-1} \\ + \lambda_1 G_i^{\mathrm{b}}(z+1,s-1|1)\langle G_i(z,s+1|r_i;[z,s])\rangle_{z+1,s-1} \end{Bmatrix} \quad (35)$$

The angle bracket terms in this equation follow from eq 27 as

$$\langle G_i(z,s+1|r_i;[z,s])\rangle_{z-1,s-1} = \begin{Bmatrix} \lambda_{-1}' G_i^{\mathrm{f}}(z-1,s+1|r_i) \\ + \lambda_0 G_i^{\mathrm{c}}(z,s+1|r_i) \\ + \lambda_1 G_i^{\mathrm{b}}(z+1,s+1|r_i) \end{Bmatrix} \quad (36)$$

with similar definitions for the other terms in eq 35.

The calculations for volume fraction profiles of all components are performed in the same manner as outlined Appendix III of Evers *et al.*[3] For cases with backfolding allowed, the solution strategy is exactly the same. For cases with backfolding prohibited, the calculations employ the conditional weighting factors and modified normalization constants defined in this work for the molecules that are longer than two segments.

As shown in Appendices I and II, branched polymers can be treated using the same basic ideas, although the computational complexity increases significantly. If we were to develop computer code following the usual procedural programming approach, we would need $2(2b + 1)$ matrices to store conditional weighting factors for a backfolding chain with b branches, and $6(2b + 1)$ matrices for a corresponding nonbackfolding chain. Furthermore, we would need to generate new code for each molecular architecture that we wished to study. We avoided these problems by implementing an object-oriented programming scheme to model both linear and branched molecules. Next, we present results that show the effect of allowing or prohibiting backfolding for various cases of linear and branched homopolymers and copolymers.

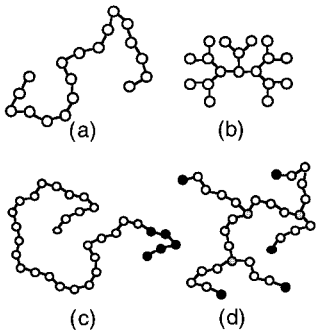

Figure 2. Architectures of the different molecules considered in this work: (a) 18 segment linear homopolymer; (b) 18 segment dendrite-like branched homopolymer; (c) 32-segment linear copolymer with 27 A segments and 5 B segments; (d) 32-segment branched copolymer with 27 A segments and 5 B segments.

III. Results and Discussion

We denote the polymer−solvent interaction parameter as χ_{A0}. The polymer−surface interaction parameter, χ_{AS}, is related[3] to the adsorption energy u_A^s/kT of Scheutjens and Fleer[2] through $u_A^s/kT = \lambda_1\chi_{AS}$. In all cases, the calculations employ a cubic lattice and assume that the polymers are monodisperse and of a single type (i.e., no mixtures).

III.A. Homopolymer Adsorption. First, we consider the adsorption of homopolymers from solution onto an adsorbing surface from dilute solution. We will examine the effect of no backfolding on the architecture of the molecule. We consider two architectures: a linear polymer and a highly branched dendritic polymer. For simplicity of creating a multiply branched molecule, we consider the case of an 18-segmented dendrite-like molecule. In order for the comparison to be reasonable, we use the same number of segments in the linear molecule. The comparison between the low-molecular weight 18-segment linear (Figure 2a) and dendrite-like branched polymers (Figure 2b) will indicate the maximum effect of backfolding correction.

Figure 3 shows the polymer volume fractions for the linear and branched polymers under both backfolding and nonbackfolding conditions. The polymer−solvent and polymer−surface interaction parameters are $\chi_{A0} = 0$ and $\chi_{AS} = -1$, respectively, indicating good solvent conditions and relatively weak polymer adsorption. The layer number increases with distance away from the surface. The volume fraction profiles for the two polymer architectures have the same qualitative features. The low adsorption energy and the good solvent conditions lead to surface depletion in all cases. When backfolding is permitted, the small polymer−surface

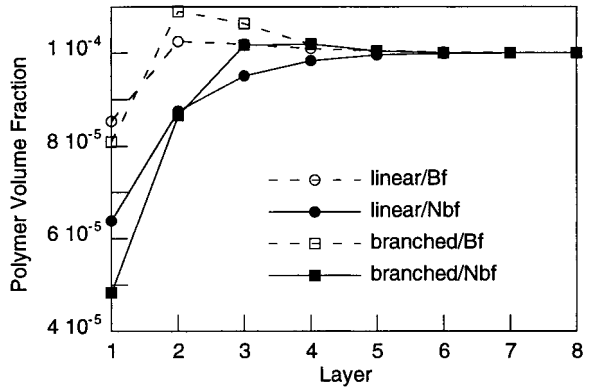

Figure 3. Spatial distributions of polymer volume fraction near a weakly adsorbing surface for linear and dendrite-like branched homopolymers of 18 segments, for both backfolding (Bf) and nonbackfolding (Nbf) conditions. Parameters include $\chi_{A0} = 0$, $\chi_{AS} = -1$, and $\phi_p^b = 1.0 \times 10^{-4}$.

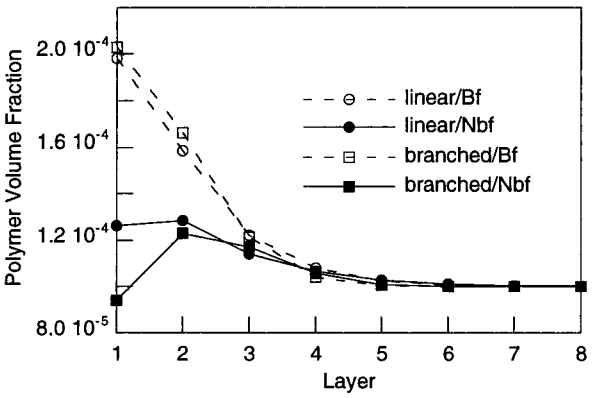

Figure 4. Spatial distributions of polymer volume fraction near a weakly adsorbing surface for linear and dendrite-like branched homopolymers of 18 segments, for both backfolding (Bf) and nonbackfolding (Nbf) conditions. Parameters include $\chi_{A0} = 0.5$, $\chi_{AS} = -1$, and $\phi_p^b = 1.0 \times 10^{-4}$.

attraction favors configurations leading to a slight maximum in the profile. The profile for the branched polymer displays a more pronounced maximum because its comparatively compact architecture keeps its segments near the surface. Furthermore, it sacrifices less configurational entropy upon adsorption compared to the linear polymer.

Prohibition of backfolding intensifies the surface depletion and increases the length scale over which the volume fractions differ between the two chain architectures. The surface volume fraction decreases by 25% for the linear polymer and 40% for the branched polymer. These observations indicate that the effect of prohibiting backfolding varies with the molecular architecture.

If we make the solvent a marginal one for the polymer by increasing χ_{A0} to 0.5, the amount of polymer adsorption increases as expected (Figure 4). With backfolding allowed, we observe that the volume fraction profiles decrease monotonically away from the surface. Again, architectural and entropic factors lead to a slightly higher volume fraction of the branched polymer near the surface. With backfolding prohibited, the profiles have a qualitatively different shape with decreased surface volume fractions and volume fraction maxima away from the surface. These results indicate that the assumption of backfolding can give qualitatively different predictions with respect to surface adsorption or depletion.

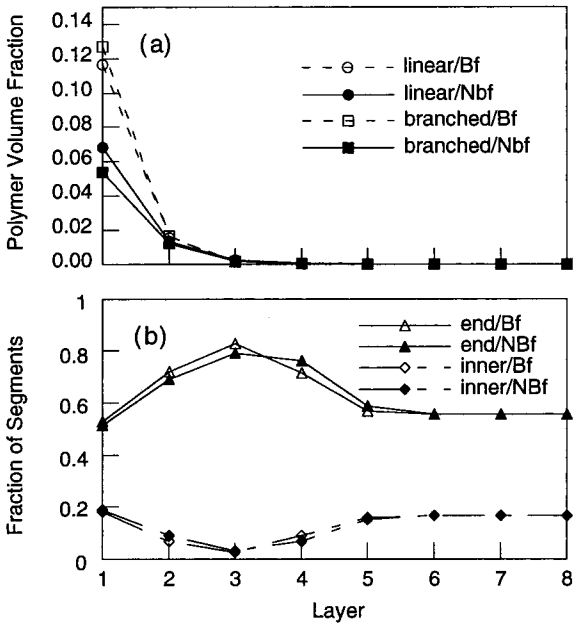

Figure 5. Spatial distributions in polymer volume fraction near a strongly adsorbing surface for linear and branched homopolymers of 18 segments, for both backfolding (Bf) and nonbackfolding (Nbf) conditions. Parameters include $\chi_{A0} = 0$, $\chi_{AS} = -5$, and $\phi_p^b = 1.0 \times 10^{-4}$. (a) Total volume fractions. (b) Distribution of the end-segments and inner-segments of the branched polymer expressed as fractions of the total branched polymer volume fraction.

Figure 4 shows again that the effect of backfolding on layer structures varies with the chain architecture. In particular, prohibiting backfolding has a greater effect on the branched polymer than on the linear polymer. In going from backfolding to nonbackfolding conditions, the branched polymer goes from being the most strongly adsorbed to being the most strongly depleted. At larger distances from the surface, chain architecture dominates the volume fraction profiles more than the backfolding condition.

We can readily rationalize these observations. The adsorption of one segment of the branched polymer at the surface increases the probability of finding its remaining segments near the surface because the molecule may span no more than seven layers. The linear molecule, on the other hand, may span up to 18 layers. This explains the higher surface volume fraction of the branched polymer when we permit backfolding. When we prohibit backfolding, volume exclusion by an adsorbed segment decreases the probability of adsorbing its nearest-neighbor segments. This has a greater effect on the branched polymer because each of its segments has more nearest-neighbors than the linear polymer. Furthermore, the linear polymer may assume loop conformations that, despite the enhanced volume exclusion, increase the surface volume fraction.

We observe similar effects in Figure 5a for stronger adsorption ($\chi_{AS} = -5$) from a good solvent ($\chi_{A0} = 0$). In going from backfolding to nonbackfolding conditions, the surface volume fraction decreases by as much as 60% for both branched and linear polymers. With backfolding, the branched polymer has a greater surface volume fraction than the linear polymer. When we prohibit backfolding, the linear polymer has the greater surface volume fraction. Again, architectural features have more control over the volume fraction profile away from the surface.

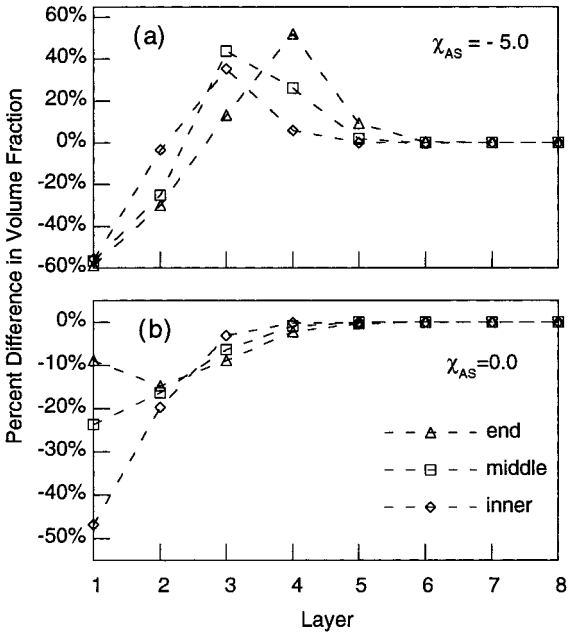

Figure 6. Percentage difference in volume fraction between nonbackfolding and backfolding cases for end, middle, and inner segments of the branched homopolymer (Figure 2b). (a) A strongly adsorbing surface with $\chi_{AS} = -5$. (b) A nonadsorbing surface with $\chi_{AS} = 0$. Other parameters include $\chi_{A0} = 0$ and $\phi_p^b = 1.0 \times 10^{-4}$.

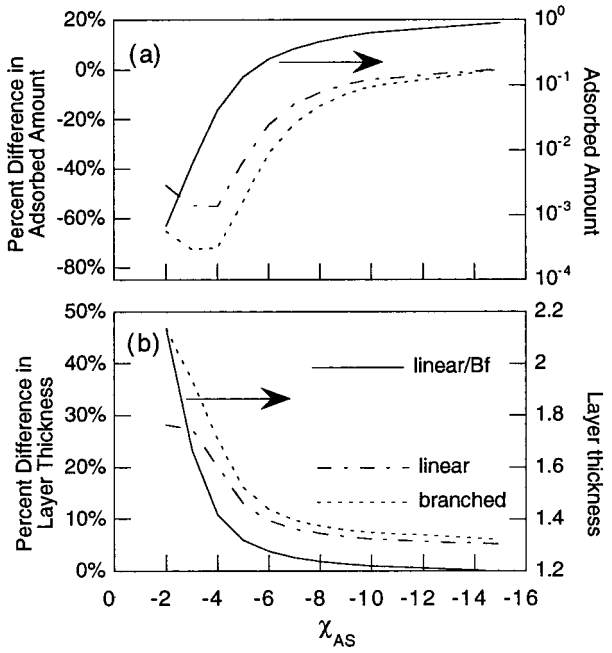

Figure 7. Percentage difference (between the nonbackfolding and backfolding cases) in the (a) adsorbed amount and (b) adsorbed layer thickness of linear polymer (dash−dot curve) and branched polymer (dotted curve) as a function of polymer−surface interaction energy. The solid curve denotes the absolute values of the adsorbed amount and layer thickness for the backfolding case. The layer thickness is in units of segment length. Other parameters include $\chi_{A0} = 0$ and $\phi_p^b = 1.0 \times 10^{-4}$.

We may differentiate among three types of segments within the branched polymer shown in Figure 2b: it includes 10 end segments (55.6% of the total, 18), five middle-node segments (27.7%), and three inner-node segments (16.7%). Figure 5b shows the distribution of the end segments and inner-node segments in the branched polymer, expressed as fractions of the total polymer volume fraction. At the surface, the fraction of end segments falls slightly below the bulk value (0.556); away from the surface, it displays a maximum. When we prohibit backfolding, the surface fraction falls from 0.53 to 0.51, and the peak shifts slightly outward. In contrast, the inner segments display preferential adsorption at the surface, but they are depleted away from the surface before reaching the bulk value (0.167). When we prohibit backfolding, the surface fraction increases from 0.18 to 0.19. Overall, we conclude that the backfolding assumption has a relatively small effect on the fractional distribution of the various parts of the branched polymer under these conditions.

Nevertheless, the absolute amount of each type of segment at any position may vary considerably between the backfolding and nonbackfolding cases. We can see this by examining the percentage change in the volume fraction of specific segments upon prohibition of backfolding (Figure 6). For a specific type of polymer segment labeled with subscript t, this quantity is

$$\Delta\phi_t(\%) \equiv 100 \times \frac{\phi_t^{nbf}(z) - \phi_t^{bf}(z)}{\phi_t^{bf}(z)} \tag{37}$$

where the superscripts bf and nbf stand for backfolding and nonbackfolding. With strong adsorption (Figure 6(a), $\chi_{AS} = -5$), prohibition of backfolding leads to similar magnitudes of surface depletion for all types of segments. These segments are distributed away from the surface as seen in the positive values of $\Delta\phi_t$, with entropic factors determining the details of the distributions of the three segment types. Figure 6(b) shows a similar plot for $\chi_{AS} = 0$. Decreasing the polymer−surface interaction energy changes the relative depletion of each segment type. As expected, the effect of volume exclusion is largest on the inner nodes.

The adsorbed amount of the polymer

$$\phi_{ads} \equiv \sum_z [\phi_p(z) - \phi_p^b] \tag{38}$$

also varies significantly with the backfolding condition. Figure 7a plots the percentage difference (dashed curves) of the values of adsorbed amount between the nonbackfolding and backfolding cases as a function of the polymer−surface interaction energy. Figure 7a also shows that adsorbed amount (solid curve) varies by orders of magnitude over this range of χ_{AS} values. The adsorbed amount typically decreases upon prohibition of backfolding. The relative difference is largest at low interaction energies and for the branched polymer, indicating that entropic factors are responsible.

The polymer layer thickness can be calculated from the first moment via

$$t \equiv \frac{2\sum_z \left(z - \frac{1}{2}\right)[\phi_p(z) - \phi_p^b]}{\phi_{ads}} \tag{39}$$

Figure 7b shows the percentage difference in the layer thickness between the nonbackfolding and backfolding cases. At low values of χ_{AS}, where the layer thickness is large, the nonbackfolding calculation predicts layer thicknesses that are as much as 46% greater than the corresponding calculation that allows backfolding. The difference is largest for the branched polymer. Again,

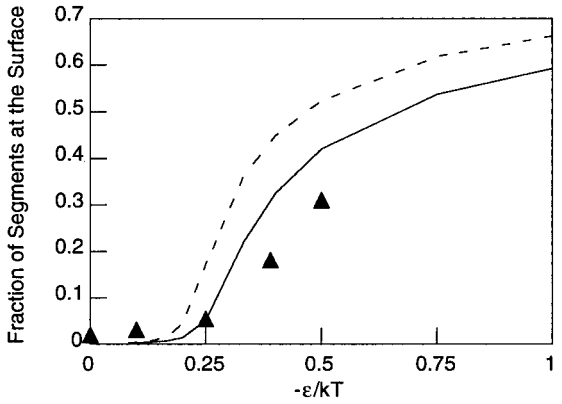

Figure 8. Surface fraction of polymer segments computed from the SCF model and Monte Carlo simulations[9] (symbols) for a linear homopolymer with 200 segments. The SCF predictions include backfolding (dashed curve) and nonbackfolding (solid curve) results. Other parameters include $\chi_{A0} = 0$ and $\phi_p^b = 1.0 \times 10^{-3}$.

entropic contributions to the configurational free energy are implicated.

The surface fraction of polymer segments may be found from

$$\gamma_0 = \frac{\phi_A(1)}{\sum_z \phi_A(z)} \tag{40}$$

McCrackin[9] has compared surface fraction values from Monte Carlo (MC) simulations with results from an early continuum self-consistent field model. In the MC simulations, ϵ represents the polymer-surface interaction energy of each segment at the surface relative to that of the solvent, so that $\chi_{AS} = \epsilon/\lambda_1 kT$.

Figure 8 compares the predictions of the lattice-based self-consistent field model with McCrackin's MC data[9] for a linear homopolymer of 200 segments. For weakly adsorbing surfaces, the surface fraction is low. The MC values of surface fraction are higher than those predicted by the SCF model because McCrackin's calculations employed chains tethered to the surface at one end. The effect of end-tethering is significant for comparisons of SCF and MC results for lower molecular weight chains but relatively unimportant for the 200 segment chain calculations shown in Figure 8. For more strongly adsorbing surfaces, the prohibition of backfolding brings the SCF model's prediction of surface fraction closer to agreement with the MC data. Merely accounting for nearest neighbor excluded volume reduces the difference in surface fraction by almost 50%. Further excluded volume corrections would probably produce less dramatic changes. This result may suggest that the most significant contribution of excluded volume effects come from the nearest segments rather than from those further along the same chain.

III.B. Copolymer Adsorption. Figure 9 shows volume fraction profiles for adsorption from solution of two copolymers of identical composition but different architecture. One is a linear A−B diblock copolymer (Figure 2c); the other is a three-branch copolymer with B segments at its ends (Figure 2d). Both copolymers have the same segment weight fraction and molecular weights, namely 5 B segments out of a total of 32 segments of A and B. The two architectures differ in the way the B segments are distributed within the

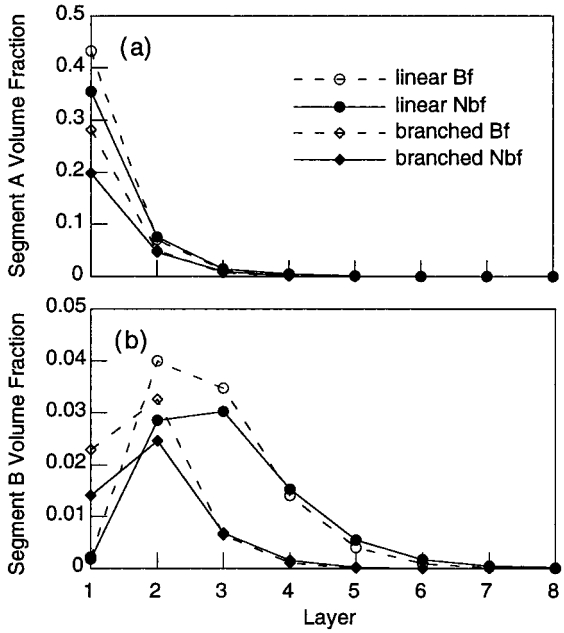

Figure 9. Spatial distributions in the segment volume fractions of linear and branched A−B copolymers containing 27 A segments and 5 B segments, for both backfolding (Bf) and nonbackfolding (Nbf) cases. Specific chain architectures are shown in parts c & d of Figure 2. (a) segment A profile and (b) segment B profile. Parameters include $\chi_{A0} = 0.6$, $\chi_{B0} = -0.3$, $\chi_{AB} = 0.7$, $\chi_{AS} = -5$, $\chi_{BS} = +5$ and $\phi_p^b = 1.0 \times 10^{-4}$.

molecule. We treat the case of poor solvency ($\chi_{A0} = 0.6$) and strong adsorption ($\chi_{AS} = -5$) for the majority A segments, and good solvency ($\chi_{B0} = -0.3$) with strong repulsion ($\chi_{BS} = +5$) for the B segments. The segment−segment interaction parameter $\chi_{AB} = 0.7$ implies that the segments are mutually repulsive. The bulk polymer solutions are dilute with a bulk volume fraction of 1.0×10^{-4}.

Figure 9a shows the volume fraction profile of strongly-adsorbing A segments near the surface. The profile shows the same qualitative trends that were observed in the homopolymer case. First, prohibiting backfolding decreases the surface volume fractions of adsorbing segments relative to the backfolding case. Second, the effect of backfolding on the polymer volume fraction profiles depends strongly on chain architecture. The surface volume fraction of the branched polymer is 28% lower than that of linear polymer under backfolding conditions, but is 39% lower when we prohibit backfolding.

The volume fraction profiles of the nonadsorbing segment B, shown in Figure 9b, support these observations. The B segment profiles display maxima because B segments do not adsorb, but they are held near the surface by adsorbing A segments. The B segments of the linear copolymer may reside away from the surface because they are in a block at the end of a long chain. The B segments in the branched copolymer, on the other hand, are held closer to the surface because they are distributed over shorter branches made up of strongly adsorbing A segments. As expected, the B segment maximum for the linear copolymer is further from the surface than that for the branched copolymer. When we prohibit backfolding, the B segment profiles stretch out further from the surface, and the maxima decrease in magnitude.

IV. Conclusions

We have presented a methodology to prohibit backfolding within the context of lattice-based self-consistent field models of inhomogeneous polymer−solvent mixtures. In one sense, this methodology brings the SCF lattice model into accord with the original form of Flory's lattice model for homogeneous polymer solutions. However, one should not view backfolding as a less-valid approximation compared to cases that prohibit backfolding. Instead, we view the backfolding and nonbackfolding cases as two valid, yet different, models of the thermodynamics of homogeneous and inhomogeneous polymer-solvent mixtures. In contrast to the van der Linden approach,[8] which explicitly weights the bond directions in a cubic lattice, our approach explicitly accounts for the availability of sites to prevent backfolding. Thus, our equations are lattice independent.

The prohibition of backfolding has a significant quantitative effect on the predicted structure of adsorbed polymer layers, at least for the low bulk polymer volume fractions considered in this work. For low surface adsorption energy, the layer structure depends on the balance between adsorption energy and the entropy loss associated with bringing the chain up to the impenetrable surface. The backfolding assumption has a profound influence on this part of the total entropy change upon adsorption. When the adsorption energy and adsorbed amounts are large, the entropy loss due to segment−segment excluded volume interactions becomes more significant. The backfolding assumption seems to have less impact on the magnitude of the total free energy change, and thus the structure of the adsorbed layer, under these conditions.

Accounting for nearest neighbor volume exclusion (i.e., prohibiting backfolding) typically decreases the predicted polymer volume fraction at the surface and the overall adsorbed amount, and increases the layer thickness, as expected. These differences become smaller as the polymer becomes more strongly attracted to the surface. Under certain conditions, surface adsorption under backfolding conditions change to depletion when we prohibit backfolding. Thus we observe both qualitative and quantitative differences in volume fraction profiles depending on whether or not we allow backfolding.

The impact of nearest neighbor volume exclusion depends considerably on chain architecture. Generally, prohibition of backfolding has a greater effect on the structure of an adsorbed layer of branched polymer than that of linear polymer. Branching points constrain multiple segments to a limited spatial region, thereby enhancing the impact of volume exclusion. The relative distributions of a chain's constituent segments, which may vary with rank (i.e., end vs. middle), connectivity (linear vs. branching), or chemistry (type A vs. type B), also depend on whether or not we allow backfolding.

Comparison with Monte Carlo simulations indicates that accounting for nearest neighbor excluded volume reduces the difference between SCF and MC predictions of surface polymer fraction by about 50%. This result indicates that significant excluded volume effects arise largely, if not mostly, due to nearest neighbor interactions.

Acknowledgment. We acknowledge the financial support of this work by the U.S. Army Research Office under Grant No. DAAH04-96-1-0422, the U.S. Department of Energy through Cooperative Agreement No. DE-FCO291ER75666, and the National Science Foundation under Grant No. CTS-9258137.

Appendix I

Our purpose here is to develop the recursive expressions for a branched chain in which backfolding is prohibited. The recursions can be viewed as "building" the chain one segment at a time from conditional weighting factors. Equations 22−24 provide conditional weighting factors for linear segments. In this appendix, we develop the expressions for conditional weighting factors for branch segments.

Consider a branched segment s joining three tails with end segments numbered as t_1, t_2, and t_3. For convenience, we refer to the tails by the same names (t_1, t_2, and t_3). Let s_1, s_2, and s_3 be the nearest segments to s on tails t_1, t_2, and t_3, respectively. Let us assume that we are building the chain toward tail t_3 through branch segment s from tails t_1 and t_2. Since segment s_3 is a linear segment, an expression similar to eq 22 provides the "forward" conditional weighting factor for s_3 as

$$G_i(z,s_3|t_1t_2;[z+1,s_3+1]) = G_i(z,s_3)\begin{Bmatrix}\lambda_{-1}G_i(z-1,s|t_1t_2;[z,s_3]) \\ +\ \lambda_0 G_i(z,s|t_1t_2;[z,s_3]) \\ +\ \lambda_1' G_i(z+1,s|t_1t_2;[z,s_3])\end{Bmatrix} \quad \text{(I.1)}$$

The notation $s|t_1t_2$ indicates that segment s is the end segment of a subchain originating from *two* points, namely segments t_1 and t_2 on the corresponding tails. Segment $s_3 + 1$ follows segment s_3 on tail t_3. The occupancy condition $[z + 1, s_3 + 1]$ is handled by the λ_1' term in the curly brackets. The conditional weighting factors $G_i(z-1,s|t_1t_2;[z,s_3])$, $G_i(z,s|t_1t_2;[z,s_3])$, and $G_i(z+1,s|t_1t_2;[z,s_3])$ are joint probabilities that end segments s of two tails t_1 and t_2 will meet at a given layer. The condition $[z,s_3]$ is imposed on the weight of segment s because segment s_3 is placed in layer z. In conformity with our earlier definition of the conditional weighting factor, the location of s_3 constrains the possible locations of s because it is a nearest neighbor, even though s_3 is not part of the subchains associated with $s|t_1t_2$. Similarly, we can readily write equations for the "central" and "backward" conditional weighting factors analogous to eqs 23 and 24.

The conditional weighting factors (CWFs) for the branch segment s can be developed in a way similar to that of the connectivity law, eq 28, for linear chains, because they account for the joint presence of segments s_1 and s_2 on tails t_1 and t_2, respectively. However unlike eq 28, additional constraints must be imposed to exclude backfolded configurations. Thus we require "forward", "central", and "backward" CWFs. We illustrate this by expanding the "central" CWF for a branch segment as

$$G_i(z,s|t_1t_2;[z,s_3]) = G_i(z,s)\begin{Bmatrix}\lambda_{-1}G_i(z-1,s|t_1;[z,s])\langle G_i(z,s_2|t_2;[z,s])\rangle_{\substack{z-1,s_1\\ z,s_3}} \\ +\ \lambda_0' G_i(z,s_1|t_1;[z,s])\langle G_i(z,s_2|t_2;[z,s])\rangle_{\substack{z,s_1\\ z,s_3}} \\ +\ \lambda_1 G_i(z+1,s_1|t_1;[z,s])\langle G_i(z,s_2|t_2;[z,s])\rangle_{\substack{z+1,s_1\\ z,s_3}}\end{Bmatrix} \quad \text{(I.2)}$$

The expansion may be interpreted as the weight of the

free segment s in layer z, multiplied by the site-weighted average of the product of CWFs for the two tails (i.e., the CWF for segment s_1 of tail t_1 with that for segment s_2).

In eq I.2, the occupancy constraint $[z, s_3]$ on segment s must be imposed on the CWFs for both segments s_1 and s_2. For s_1, it requires the λ_0' term corresponding to the exclusion of one site in layer z. For s_2, the angle brackets indicate that the CWFs are site-weighted averages, so the occupancy constraints $[z, s_3]$ are recorded as subscripts; the implications will be described below. The CWFs for s_1 and s_2 also carry the condition $[z,s]$ imposed due to the placement of nearest neighbor s in layer z.

For each placement of the segment s_1, there is a joint placement of segment s_2 in the vicinity of layer z because both s_1 and s_2 are neighbors of s. The placement of s_2 must account for all of the conditions imposed so far, namely that s_3 is in layer z, s is in layer z, and that s_1 is in an adjoining layer. Because s is the nearest neighbor of s_2 along the chain, we impose its occupancy constraint $[z,s]$ in the CWFs that make up the site-weighted averages. The occupancy constraints of the *next* nearest neighbors (to s_2) s_1 and s_3 denoted via subscripts appended to the angle brackets. The site-weighted average CWFs for segment s_2 may be written as

$$\langle G_i(z,s_2|t_2;[z,s])\rangle_{\substack{z-1,s_1\\ z,s_3}} = \begin{Bmatrix} \lambda'_{-1} G_i(z-1,s_2|t_2;[z,s]) \\ + \lambda_0' G_i(z,s_2|t_2;[z,s]) \\ + \lambda_1 G_i(z+1,s_2|t_2;[z,s]) \end{Bmatrix} \quad \text{(I.3)}$$

$$\langle G_i(z,s_2|t_2;[z,s])\rangle_{\substack{z,s_1\\ z,s_3}} = \begin{Bmatrix} \lambda_{-1} G_i(z-1,s_2|t_2;[z,s]) \\ + \lambda_0'' G_i(z,s_2|t_2;[z,s]) \\ + \lambda_1 G_i(z+1,s_2|t_2;[z,s]) \end{Bmatrix} \quad \text{(I.4)}$$

$$\langle G_i(z,s_2|t_2;[z,s])\rangle_{\substack{z+1,s_1\\ z,s_3}} = \begin{Bmatrix} \lambda_{-1} G_i(z-1,s_2|t_2;[z,s]) \\ + \lambda_0' G_i(z,s_2|t_2;[z,s]) \\ + \lambda_1' G_i(z+1,s_2|t_2;[z,s]) \end{Bmatrix} \quad \text{(I.5)}$$

The λ'_{-1} in the first term of eq I.3 accounts for the occupancy of segment s_1 in layer $z-1$ and the λ_0' in the second term of eq I.3 accounts for the occupancy of segment s_3 in layer z. In eq I.4, we use the λ_0'' term, defined by eq 9, because both s_1 and s_3 occupy the layer z. Thus, the occupancy constraints on segment s_2 due to segment s_3 in layer z and segment s_1 in adjoining layers are incorporated through λ_i' and λ_i'' terms. Expressions similar to eqs I.3 to I.4 can be written for the other terms that will appear in the "forward" and "backward" CWFs analogous to eq I.2.

The composition laws developed in Appendix II will require corresponding CWFs for the situation when the molecule is built from the branch segment s towards either tail t_2 or t_3. These expressions are analogous to those developed above.

Appendix II

In this appendix, we derive the expressions for the composition law for a branch segment that connects three subchains. We use the notation developed in Appendix I with regard to the segments near the branch segment s. The composition law for a branch segment s joining three tails t_1, t_2, and t_3 requires that we account for the joint occupancy of sites neighboring segment s by segments s_1, s_2, and s_3. Thus, we need conditional weighting factors for each of these segments that account for the constraints imposed by location of the other two segments.

The composition law defines the chain segment distribution function $G_i(z,s|t_1t_2t_3)$, which represents the combined statistical weight of all chains that have segment s (connecting subchains t_1, t_2, and t_3) in layer z. This function may also be interpreted as the joint probability of having three-node branch segment s in layer z while segments s_1, s_2, and s_3 are simultaneously in the vicinity of layer z, namely in layers $z-1$, z, and $z+1$. We can construct this joint probability as the site-weighted average of CWF products:

$$G_i(z,s|t_1t_2t_3) = G_i(z,s) \begin{Bmatrix} \lambda_{-1} G_i(z-1,s_1|t_1;[z,s]) \langle G_i(z,s_2|t_2;z,s_3|t_3;[z,s])\rangle_{z-1,s_1} \\ + \lambda_0 G_i(z,s_1|t_1;[z,s]) \langle G_i(z,s_2|t_2;z,s_3|t_3;[z,s])\rangle_{z,s_1} \\ + \lambda_1 G_i(z+1,s_1|t_1;[z,s]) \langle G_i(z,s_2|t_2;z,s_3|t_3;[z,s])\rangle_{z+1,s_1} \end{Bmatrix} \quad \text{(II.1)}$$

We first recognize that $G_i(z,s|t_1t_2t_3)$ is proportional to the free segment weight of segment s. The occupancy constraint $[z,s]$ occurs in each of the CWFs for segments s_1, s_2, and s_3 because s is the nearest neighbor of each. The distribution function is proportional to the site-weighted average of products of CWFs for the subchain ending in segment s_1 (for example, $G_i(z-1,s_1|t_1;[z,s])$) with the site-weighted joint probability for placing both segments s_2 and s_3 from subchains t_2 and t_3. The latter is represented, for example, by $\langle G_i(z,s_2|t_2;z,s_3|t_3;[z,s])\rangle_{z-1,s_1}$. No λ_i' terms are needed in the site-weighted average of eq II.1 because we place s_1 before the other connecting subchain segments. The occupancy constraints due to the location of s_1 are given as subscripts to the angle brackets because s_1 is not a nearest neighbor of segment s_2 or s_3.

We derive the joint probability $\langle G_i(z,s_2|t_2;z,s_3|t_3;[z,s])\rangle_{z-1,s_1}$ by placing segment s_2 followed by segment s_3. It can be written as the site-weighted average of the product of the CWF for segment s_2 and the site-weighted average CWF for segment s_3:

$$\langle G_i(z,s_2|t_2;z,s_3|t_3;[z,s])\rangle_{z-1,s_1} = \begin{Bmatrix} \lambda'_{-1} G_i(z-1,s_2|t_2;[z,s]) \langle G_i(z,s_3|t_3;[z,s])\rangle_{\substack{z-1,s_1\\ z-1,s_2}} \\ + \lambda_0 G_i(z,s_2|t_2;[z,s]) \langle G_i(z,s_3|t_3;[z,s])\rangle_{\substack{z-1,s_1\\ z,s_2}} \\ + \lambda_1 G_i(z+1,s_2|t_2;[z,s]) \langle G_i(z,s_3|t_3;[z,s])\rangle_{\substack{z-1,s_1\\ z+1,s_2}} \end{Bmatrix} \quad \text{(II.2)}$$

Equations similar to eq II.2 can be written for the other terms in eq II.1. As before, the subscripts on the angle brackets indicate occupancy constraints due to next-nearest neighbors. The λ'_{-1} term in eq II.2 accounts for the presence of segment s_1 in layer $z-1$ which constrains the placement of segment s_2 in that layer. The joint placement of segment s_3 introduces the site-weighted average CWF for segment s_3. The locations of segments s_1 and s_2 constrain the placement of s_3 and so are represented as subscripts on angle brackets.

The site-weighted average CWFs for segment s_3 can be related to the corresponding CWFs for each layer through expressions analogous to eqs I.3−I.5. For

example, we have

$$\langle G_i(z,s_3|t_3;[z,s])\rangle_{\substack{z-1,s_1\\z-1,s_2}} = \left\{\begin{matrix}\lambda''_{-1}G_i(z-1,s_3|t_3;[z,s])\\ +\lambda_0 G_i(z,s_3|t_3;[z,s])\\ +\lambda_1 G_i(z+1,s_3|t_3;[z,s])\end{matrix}\right\} \quad \text{(II.3)}$$

The λ''_{-1} term, defined in eq 9, accounts for the occupancy of segments s_1 and s_2 in layer $z-1$. Similar expressions will be required for the site-weighted average CWFs that appear in the equations for $\langle G_i(z,s_2|t_2;z,s_3|t_3;[z,s])\rangle_{z,s_1}$ and $\langle G_i(z,s_2|t_2;z,s_3|t_3;[z,s])\rangle_{z+1,s_1}$ in eq II.1.

References and Notes

(1) Flory, P. J. *Principles of Polymer Chemistry*; Cornell University Press: New York, 1953.
(2) Scheutjens, J. M. H. M.; Fleer, G. J. *J. Phys. Chem* **1979**, *83*, 1619.
(3) Evers, O. A.; Scheutjens, J. M. H. M.; Fleer, G. J. *Macromolecules* **1990**, *23*, 5221.
(4) Theodorou, D. N. *Macromolecules* **1988**, *21*, 1400.
(5) Theodorou, D. N. *Macromolecules* **1989**, *22*, 4578.
(6) Hariharan, A.; Kumar, S. K. *J. Chem. Phys.* **1993**, *98*, 6516.
(7) Leermakers, F. A. M.; Scheutjens, J. M. H. M. *J. Chem. Phys.* **1988**, *89*, 3264.
(8) van der Linden, C. C.; Leermakers, F. A. M.; Fleer, G. J. *Macromolecules* **1996**, *29*, 1172.
(9) McCrackin, F. L. *J. Chem. Phys.* **1967**, *47*, 1980.

MA980170K